



Quantitative and qualitative saccharide analysis of North Atlantic brown seaweed by gas chromatography/mass spectrometry and infrared spectroscopy

Calle Niemi ^a, Junko Takahashi ^b, András Gorzsás ^c, Francesco G. Gentili ^{a,*}

^a Department of Forest Biomaterials and Technology, Swedish University of Agricultural Sciences, Umeå 901 83, Sweden

^b Department of Forest Genetics and Plant Physiology, Umeå Plant Science Centre, Swedish University of Agricultural Sciences, Umeå 901 83, Sweden

^c Vibrational Spectroscopy Core Facility, Department of Chemistry, Umeå University, Umeå 90187, Sweden

ARTICLE INFO

Keywords:

Alginate
FTIR
GC/MS
MG ratio
North Atlantic brown seaweed

ABSTRACT

Brown seaweeds contain a variety of saccharides which have potential industrial uses. The most abundant polysaccharide in brown seaweed is typically alginate, consisting of mannuronic (M) and guluronic acid (G). The ratio of these residues fundamentally determines the physicochemical properties of alginate. In the present study, gas chromatography/mass spectrometry (GC/MS) was used to give a detailed breakdown of the monosaccharide species in North Atlantic brown seaweeds. The anthrone method was used for determination of crystalline cellulose. The experimental data was used to calibrate multivariate prediction models for estimation of total carbohydrates, crystalline cellulose, total alginate and alginate M/G ratio directly in dried, brown seaweed using three types of infrared spectroscopy, using relative error (RE) as a measure of predictive accuracy. Diffuse reflectance infrared Fourier transform spectroscopy (DRIFTS) performed well for the estimation of total alginate (RE = 0.12, R² = 0.82), and attenuated total reflectance (ATR) showed good prediction of M/G ratio (RE = 0.14, R² = 0.86). Both DRIFTS, ATR and near infrared (NIR) were unable to predict crystalline cellulose and only DRIFTS performed better in determining total carbohydrates. Multivariate spectral analysis is a promising method for easy and rapid characterization of alginate and M/G ratio in seaweed.

1. Introduction

Seaweeds represent a rich source of compounds and materials which have a wide array of uses [1]. They contain numerous complex carbohydrates including several types of dietary fibers which have potential health benefits [2], and which have structural properties which make them useful for industrial purposes. Carbohydrates often represent the largest component of seaweed biomass by dry weight (DW), sometimes as much as 70 % in brown seaweed [3]. Understanding and characterizing the polysaccharide contents of seaweed biomass is important for estimating their chemical properties and consequently their potential uses [19].

The unique gelling qualities of many seaweed polysaccharides have led to them being used for thickening or binding in many common food items as well as being used in a variety of research fields and for medical purposes [1,4–6]. Brown seaweed contains a number of unique polysaccharides, including fucoidan, laminarin and alginate. Fucoidan, as

the name implies, consists largely of fucose, but with occasional sulfate-modifications. The minor monosaccharides, xylose, galactose, arabinose and rhamnose, can be also found in fucoidan along with fucose as the main sugar in the backbone [7]. Laminarin is a seaweed-specific storage glucan consisting of glucose residues bound together by β -1,3- bonds, with branching β -1,6- bonds [8]. The most abundant polysaccharide, and often the most abundant biomolecule in brown seaweed in general, is alginate [3]. Alginate is a polymer largely specific to brown seaweeds, which is currently used in several industries, particularly for biodegradable food packaging [9]. Alginate and other seaweed phycocolloids are optimal for use as biodegradable films for foods such as fruits, as they are edible, impermeable to oxygen, prevent microbial contamination, and protect the food during transportation [10]. Alginate is also commonly used in the dental industry for taking dental imprints for diagnosis or to be used as molds for prosthetic implants [11]. More recently, the potential for using alginate as a 3D-printing material has also been investigated [12], including the production of 3D-printed

* Corresponding author.

E-mail address: francesco.gentili@slu.se (F.G. Gentili).

<https://doi.org/10.1016/j.ijbiomac.2023.127870>

Received 18 April 2023; Received in revised form 16 September 2023; Accepted 1 November 2023

Available online 13 November 2023

0141-8130/© 2023 The Authors. Published by Elsevier B.V. This is an open access article under the CC BY license (<http://creativecommons.org/licenses/by/4.0/>).

agar/alginate-supported hydrogels used as scaffolds for bioprinting of live cells for tissue reconstruction [13]. The production of biodegradable plastics incorporating alginate is also being investigated [14].

In addition to the interesting structural uses for alginate, it also has the ability to chelate metal ions which has proven to be useful for wastewater remediation. It has been shown that alginate can be used to remove heavy metal contaminants from wastewater streams, including Pb^{2+} , Cu^{2+} , Cd^{2+} , and that these metals can be recovered from the resulting alginate gel by calcination at elevated temperatures, resulting in metal oxide nanopowders [15]. Furthermore, alginate contains a large number of hydroxylic and carboxylic moieties which can be chemically modified, enabling vast customization of its physicochemical properties [16]. This further indicates the variety of uses for seaweed polymers. Comprising as much as 30–45 % of the total DW of certain brown seaweed species [3], alginate is a very abundant material, suitable for industrial-scale production. Seaweeds are rapid-growing and naturally occurring in a wide range of geographical areas, and its cultivation and harvest on industrial scale is expanding [17].

Structurally speaking, alginate is a linear polymer consisting of the uronic acid residues β -D-mannuronic (M) and α -L-guluronic (G) acid [18]. The ratio and distribution of the M and G residues within the linear chain determines the physicochemical properties of the polymer, so these factors must be considered when using alginate for specific industrial processes [19]. The M and G monomers can be found either in hetero blocks (mixed M and G), M-blocks (stretches of just M-residues) or G-blocks (stretches of G-residues), which heavily influences the rigidity of the resulting gel or film. The C1 and C4 glycosidic bonds within G-blocks have an equatorial conformation which places the carboxylic moieties in a position that facilitates alginate's binding of metal ions (commonly Na^+ , Ca^{2+} , Mg^{2+} , Sr^{2+} , Ba^{2+}) in a so-called egg-box structure [9,18]. The glycosidic bonds of M-blocks on the other hand have an axial formation which does not form an ion-binding site. The binding of divalent metal ions in G-blocks enhances the rigidity of the gel, as the electrostatic interactions between the anionic charges of the alginate fiber and the cationic charges of the metal ions allow for intermolecular ionic crosslinking. The M/G ratio is thus one of the main factors determining the properties of alginate gel. This ratio is typically decided through time-consuming methods involving partial hydrolysis and ^1H liquid-state Nuclear Magnetic Resonance (NMR) spectroscopy or ^{13}C NMR, or colorimetric estimations, but it has been shown that the M/G ratio of extracted alginate can also be estimated more rapidly through infrared spectroscopic methods [20,21]. Estimation of M/G ratios directly in brown seaweed has also been performed by calculating ratios between specific absorbance bands in the infrared spectrum [22]. Fourier transform infrared spectroscopy (FTIR) in particular has been used more and more frequently in the last two decades to study alginate, and spectral characterization of seaweed polysaccharides is a growing field of study [23–26].

In the present study, the carbohydrate profiles of four species of brown seaweed from the North Atlantic region are determined, namely *Alaria esculenta*, *Saccharina latissima*, *Laminaria digitata*, and *Himantalia elongata*, and this experimental data is used to assess the viability of spectral methods for estimating carbohydrates in seaweed. Seaweeds from primarily Norway and the Faroe Islands are characterized, with a few additional samples from Ireland and Greenland. Crystalline cellulose contents are estimated by the Updegraff method and anthrone assay. The total carbohydrate and alginate content as well as detailed monosaccharide composition is estimated by complete sulfuric acid hydrolysis of polysaccharides followed by identification and quantification of monosaccharide species using gas chromatography/mass spectrometry (GC/MS). Moreover, the GC/MS technique was used to quantify M and G contents in the seaweeds, which to the authors' knowledge has not been done previously. The potential for using infrared spectroscopic techniques coupled with multivariate analysis to estimate total carbohydrate, total crystalline cellulose, total alginate contents and the alginate M/G ratio directly in brown seaweed biomass

is investigated, using three different spectroscopic techniques and partial least squares regression (PLSR) multivariate analysis. The validity of PLSR predictions is assessed through identification of relevant spectral bands in the regression coefficients of the resulting models. This study therefore serves to show that alginate and M/G ratio can be estimated from brown seaweed biomass without the need for chemical characterization methods.

2. Material and method

2.1. Sampling and pre-processing of seaweed

The seaweed samples used in the present study have been described in detail previously [27]. Briefly, all samples were dried by either hot-air drying or freeze-drier, and shipped to Umeå, Sweden, for milling and analysis. Samples were milled using a 400 MM Mixer Mill (Retsch GmbH, Haan, Germany) until the whole sample could pass through a 250 μm sieving screen, to ensure small enough particles for efficient extraction. In total, 38 samples of brown seaweed, mostly from the Faroe Islands as well as Tromsø and Bodø in Norway, were analyzed. Biological replicates per species and location are shown in Table 1.

2.2. Updegraff cellulose and anthrone assay

Amorphous polymers and soluble sugars were removed from samples by suspension of 3 (± 0.2) mg algal powder in 1.5 mL Updegraff reagent [28], consisting of acetic acid:nitric acid:water in a 8:1:2 ratio (v/v). Samples were heated at 100 °C for 30 min, and allowed to cool down to room temperature before being centrifuged at approx. 18,700 $\times g$ for 10 min at 15 °C. The supernatant was removed, and the pelleted cellulose was washed once with 1.5 mL water and once with 1.5 mL acetone, by centrifuging as previously described. The pellet was dried under vacuum overnight.

Saeman hydrolysis was used to break down the crystalline cellulose into glucose [29], by suspension 72 % sulfuric acid (H_2SO_4). Samples were shaken for 30 min, sonicated for 15 min, and shaken for another 15 min. Water was added to dilute the acidic sample, and 20 μL was used for colorimetric quantification using the anthrone assay (Scott and Melvin, 1953). The sample hydrolysate was diluted in deionized water to a total volume of 200 μL , and the same was done with a glucose standard curve of 0, 25, 50 and 100 $\mu\text{g mL}^{-1}$. To both samples and standards, 400 μL 0.2 % anthrone reagent in concentrated sulfuric acid (w/v) was followed by immediate vortexing. Samples were kept under aluminum foil to avoid photodegradation. Samples were heated at 100 °C for 5 min, and cooled down on ice. The absorbance was measured at 620 nm using an Epoch 2 microplate spectrophotometer (BioTek, Winooski, Vermont, U.S.), and the glucose standard curve was used to calculate glucose, and by extension cellulose in the samples.

2.3. Trimethylsilyl (TMS)-derivatization and GC/MS analysis of monosugar residues

For the determination of total monosaccharide residues in the seaweed samples, 500 (± 30) μg sample was pelleted using a glass capillary (Microcaps, Drummond Scientific Company, Broomall, U.S.), in quadruplicate for each sample and 30 μg inositol was added as internal standard. The monosaccharide standards, consisting of arabinose, rhamnose, fucose, xylose, glucuronic acid, galacturonic acid, mannose, glucose and galactose (Merck KGaA, Darmstadt, Germany) as well as the two alginate residues mannuronic (Merck KGaA) and guluronic acid (MCE, Princeton, NJ, USA) were prepared in 10, 20, 50 and 100 μg per each monosaccharide, except for the M and G monosaccharides, for which only 20, 50 and 100 μg were used, since these were expected to be highly abundant and did not need the lowest data point. The water from the standards was evaporated by sparging with N_2 gas in a heating block at 60 °C for 15–30 min, until fully dry. For complete polysaccharide

Table 1
Carbohydrate contents and sample numbers of analyzed brown seaweeds.

Species	Region	Sample number	Total carbohydrates	Cellulose	Alginate	M:G ratio
<i>A. esculenta</i>	Bodø	3	33.4 ± 3.8	3.6 ± 0.1	27.3 ± 2.2	5.3 ± 0.8
	Tromsø	3	37.3 ± 2.5	2.1 ± 0.4	29.8 ± 1.8	3.9 ± 0.6
	Faroe Islands	9	37.3 ± 8.5	2.8 ± 0.6	26.4 ± 5.4	2.4 ± 0.5
	Ireland	3	59.1 ± 2.2	4.6 ± 1.3	43.8 ± 5.5	3.9 ± 1.2
	Greenland*	1	31.9 ± 4.9	4.7 ± 0.2	20.9 ± 3.8	3.8 ± 0.4
<i>H. elongata</i>	Faroe Islands	3	30.6 ± 3.1	2.3 ± 0.2	21.7 ± 3.0	2.5 ± 0.1
<i>L. digitata</i>	Bodø	3	51.3 ± 5.8	4.5 ± 0.8	42.6 ± 5.5	3.0 ± 0.1
	Tromsø	3	40.3 ± 6.2	4.2 ± 0.3	30.1 ± 5.6	2.9 ± 0.5
	Faroe Islands*	1	48.0 ± 1.7	5.6 ± 1.0	34.0 ± 1.2	4.7 ± 0.3
<i>S. latissima</i>	Bodø	3	39.9 ± 0.7	3.6 ± 0.7	32.4 ± 0.1	4.9 ± 0.6
	Tromsø	3	60.3 ± 7.9	4.7 ± 0.9	45.1 ± 7.0	7.0 ± 1.7
	Faroe Islands	3	19.1 ± 3.0	2.9 ± 2.3	12.2 ± 1.6	2.5 ± 0.5

All units are in %DW, except the M/G ratio. The SD of technical and biological replicates is reported, except for the single-replicate samples labeled with *, for which only the SD of technical replicates are reported.

hydrolysis, 72 % sulfuric acid was added to all samples and standards, followed by sonication for 30 min. The hydrolysates were incubated at room temperature for 2 h. The acidic hydrolysate was diluted with ultrapure water, and the slurry was boiled at 100 °C for 150 min. After cooling down, the hydrolysates were centrifuged at approx. 18,700 ×g for 5 min, and the supernatant was collected for further processing.

The acidic hydrolysates were neutralized by addition of calcium carbonate (CaCO₃). The samples were centrifuged at 18,700 ×g for 10 min and the supernatant was collected. To further clear up the samples, centrifugation was repeated and the supernatant was collected to 6 mL glass tube, which was then dried by sparging with N₂ gas in a heating block at 60 °C, and in a vacuum chamber with phosphorus pentoxide desiccant overnight, to ensure minimal water content for the following methanolysis. 600 µL 2 M HCl/MeOH was added as methanolysis reagent, flushed briefly with N₂ gas, the cap was screwed on and the samples were incubated at 85 °C for 24 h.

The solvent was evaporated by sparging with N₂ at 40 °C. The dry sugars were washed twice with 300 µL methanol, evaporating the methanol between washes as previously described. Silylation of the methanolysed monosaccharide residues [30] was performed by addition of 200 µL silylating reagent (85,431; Merck KGaA), followed by heating at 80 °C for 20 min. The tubes were allowed to cool, and most of the solvent was evaporated under a stream of N₂. The pellet was dissolved in 1 mL hexane, centrifuged at 18,700 ×g for 5 min and filtered through glass wool. The filtrate was concentrated down to approx. 100–200 µL of which 0.5 µL was used for quantification by GC/MS (7890A/5975C; Agilent Technologies, Santa Clara, U.S.) [30]. The separation of silylated monosaccharides were performed on a J&W DB-5MS column (30 m length, 0.25 mm diameter, 0.25 µm film thickness; Agilent Technologies, Santa Clara, U.S.) with the oven program: 80 °C followed by a temperature increase of 20 °C/min to 140 °C, holding for 2 min, then 2 °C/min to 200 °C, holding for 5 min, then 30 °C/min to 250 °C for 5 min. The total run time was 47 min.

Raw data MS files from GC/MS analysis were converted to NetCDF format in Agilent Chemstation Data Analysis (Version E.02.00.493) and exported to RDA (version 2016.09; Swedish Metabolomics Centre (SMC), Umeå, Sweden). Data pretreatment procedures, such as baseline correction and chromatogram alignment, peak deconvolution and peak integration followed by peak identification was performed in RDA. Certain peaks associated with M and G residues overlapped with other monosaccharides within the standard mixture, which was confirmed by running these standards separately. Most notably, the highest-intensity M peak between 1116.4 and 1127.7 s overlapped with two minor un-specific peaks from other monosaccharide standards. This overlap could not be fully eliminated, but it was reduced by selectively integrating 216.5–217.5 *m/z*, as the 217 *m/z* ion fragment was the major fragment in M while being less pronounced in these two minor peaks (Supplementary Fig. 1a–b). The brown seaweed samples barely showed indication of these peaks after deconvolution, indicating little influence in

quantification of M residues. Further, the most intense galactose peak, the alpha-pyranosyl (α-p) peak between 1262.5 and 1276.5 s, overlapped heavily with G and M, making it unsuitable for quantification in brown seaweed samples (Supplementary Fig. 1c). The beta-pyranosyl (β-p) peak between 1338.7 and 1353.9 s also overlapped with a signal from M residues, but this overlap was eliminated by selectively integrating mass fragments between 203.5 and 204.5, as the 204 *m/z* ion fragment was unique to β-p galactose (Supplementary Fig. 1d). This peak was thus used for galactose quantification.

2.4. Infrared spectroscopies

2.4.1. Diffuse reflectance infrared Fourier transform spectroscopy (DRIFTS)

DRIFTS was evaluated as a potential method for polysaccharide analysis in dried macroalgae. Measurements were carried out using a previously established protocol [27,31]. DRIFTS measurements were performed using an IFS 66 v/S vacuum spectrometer (Bruker Optik GmbH, Ettlingen, Germany) on dried seaweed samples mixed with KBr in an approximate 1:10 sample:KBr ratio by volume. Spectra were recorded over the region of 4000–400 cm⁻¹ at a resolution of 4 cm⁻¹, co-adding 128 scans per sample with pure KBr subtracted as background using the manufacturer's software (OPUS, version 5, Bruker Optik GmbH). Spectra were processed using the MCR-ALS GUI, available at the Vibrational Spectroscopy Core Facility, Department of Chemistry, Umeå University (v4c, <https://www.umu.se/en/research/infrastructure/vi-sp/downloads/>) in MATLAB (version R2017b, MathWorks, Natick, MA, USA). The 800–1800 cm⁻¹ fingerprint region contains spectral bands that are strongly correlated to basic biochemical components found in algal biomass, including carbohydrates, and further analysis was limited to this region. All spectra were baseline corrected using asymmetric least squares (AsLS) (lambda = 20,000, p = 0.001), and subsequently normalized over the total area of the cut spectral range. Processed DRIFTS spectra were used for PLSR modeling to predict total carbohydrates, cellulose, total alginate and alginate M/G ratio in seaweed.

2.4.2. Attenuated total reflectance Fourier transform spectroscopy (ATR)

ATR FTIR spectra were recorded in the same range and with the same resolution as DRIFTS spectra, using a Vertex 80v FT-IR vacuum spectrometer (Bruker, GmbH). As ATR spectral intensities vary as a function of wavenumbers, baseline correction by AsLS may be suboptimal. Thus, ATR spectra were baseline-corrected in OPUS (version 7, Bruker Optik GmbH) using the built-in 64-point rubberband option, excluding CO₂ bands. After baseline correction, the spectra were cut to the 800–1800 cm⁻¹ range, total area normalized and used for predictive modeling in the same way as the DRIFTS spectra.

2.4.3. Near-infrared spectroscopy (NIR)

NIR analysis was performed as described previously [27]. In brief, NIR spectra of dried seaweed was captured between 350 and 2500 nm at a resolution of 1 nm using a LabSpec ASD NIR spectrophotometer (Portable Analytical Solutions, Copacabana, NSW, Australia) equipped with a contact probe. Background was removed by blanking with Spectralon white Teflon reference blank supplied by the manufacturer. The visible spectrum was removed, and spectral analysis was limited to 1000–2500 nm, followed by normalization using standard normal variate (SNV) correction. Spectra were averaged over three measurements per sample. Processing was done using Evince software (Pre-diktera AB, Umeå, Sweden).

2.5. Partial least squares regression (PLSR)

Multivariate prediction modeling with spectral data was performed using PLSR, using a method described in Niemi, Mortensen, Rautenberger, Matsson, Gorzdas and Gentili [27]. Briefly, 30 out of 38 samples were selected by random number generation to be used as calibration samples. PLSR prediction models were created from these calibration samples using RStudio Desktop software (RStudio, Boston, Massachusetts, U.S.) with scripts from the PLS package (v. 2.8–0, <https://CRAN.R-project.org/package=pls>). The optimal component number for each predicted compound and spectroscopic method was determined by leave-one-out cross-validation, and the component with the lowest RMSE of cross-validation was chosen. The models were used to predict the total carbohydrates, total cellulose, total alginate, and alginate M/G ratios of the remaining 8 samples. The accuracy of prediction for all four predicted variables was evaluated in terms of the root mean square error of prediction (RMSEP), the relative error (RE) and the correlation coefficient R^2 when comparing known values to predicted values.

3. Results and discussion

3.1. Crystalline cellulose

Crystalline cellulose contents were determined by the Anthrone assay after removal of amorphous and soluble sugars. In the four species investigated, small quantities of crystalline cellulose were detected, between 2.1 and 4.7 %DW (Table 1). Crystalline cellulose was therefore a minor component of the total carbohydrate profile, compared to alginate as shown by GC/MS. Cellulose contents in all seaweed samples were low compared to higher plant sources of cellulose, including terrestrial energy crops like *Miscanthus* and pine trees but also aquatic weeds like cattail, where cellulose is a primary component of the cell wall and can comprise close to or >40 % of the DW [32]. This seaweed cellulose would thus be of limited industrial use as it can be harvested in larger quantities from other, readily available crops.

3.2. Total carbohydrates and monosaccharide profile

The sum of monosaccharide residues determined by TMS of seaweed hydrolysates and GC/MS analysis was used to estimate the total carbohydrate content. The assayed brown seaweed samples ranged in total carbohydrates from approx. 19.1–60.3 % by DW, showing major differences between species but also regional differences (Table 1). *A. esculenta* from most regions included in this study contained between 31.9 and 37.3 %, but the Irish *A. esculenta* had notably higher contents at 59.1 %. Similarly high carbohydrate contents were measured in the *S. latissima* samples from Tromsø, at 60.3 %. The Bodø *S. latissima* samples contained 39.9 % carbohydrates, considerably lower than the Tromsø ones, despite also originating on the Norwegian coast. The Faroese *S. latissima* seaweed had the lowest carbohydrate contents by far at 19.1 %, exhibiting a wide variation within this species potentially depending on growth region. The *L. digitata* samples from both Bodø, Tromsø and the Faroe Islands contained high quantities at 51.3, 40.3 and

48.0 %, respectively. Faroese *H. elongata* had a carbohydrate content of 30.6 %.

Regarding the monosaccharide profiles, all monosugar hydrolysates largely consisted of the two alginate uronic acid residues, comprising approx. 65–86 % of the total monosaccharides by weight (Fig. 1). The third most abundant monosaccharide was glucose, in the range of 10.5–22.4 %DW. Glucose-based polysaccharides besides cellulose, like laminarin and starch, were not specifically measured, but based on existing literature it can be inferred that the majority of non-cellulose glucose residues identified in the samples stem from laminarin, as this is the primary carbon-storage molecule in brown seaweed as opposed to starch [33]. Besides glucose, all samples contained some amount of fucose, approx. 1.4–5.4 %DW in *A. esculenta*, *L. digitata* and *S. latissima*, with *H. elongata* standing out with 13.8 %DW. This fucose was likely stemming from fucoidan. While not exceedingly high in quantity in these samples, fucoidan and laminarin have both been suggested to have potential health benefits and pharmaceutical uses [7,8], and so these polysaccharides also have potential use as high-value extractives in these seaweeds.

Mannose and galactose were also present in minor quantities, approx. 1.2–3.0 and 0.7–2.2 %DW, respectively. Arabinose, rhamnose, xylose, galacturonic acid and glucuronic acid were largely <1 %DW with the exception of the Faroese *S. latissima* which contained 2.1 % galacturonic acid and 2.5 % glucuronic acid.

3.3. Alginate contents and M/G ratios

Presuming that the vast majority of M and G residues are present in their polymer form, the total alginate content was estimated from GC/MS measurements of these two monosaccharides. These monosaccharides are not typically measured using GC/MS, but the M and G standards used for calibration and identification of GC/MS data showed strong correlation between signal intensity and concentration, with R^2 values at 0.9729 and 0.9769, respectively, indicating the suitability of this method of detection (Supplementary Fig. 2). The validity of the M and G standards was further confirmed by comparing to an alginate standard (A7003; Merck KGaA) processed and analyzed in triplicate using the same procedure as the seaweed samples. The peaks of the M and G standards were confirmed to share positions with the alginate standard (Supplementary Fig. 1).

Alginate was thus estimated to a range of 12.2–45.1 %DW for the samples in this study, typically proportional to the aforementioned carbohydrate contents (Table 1). The Tromsø *S. latissima*, Irish *A. esculenta* and Bodø *L. digitata* samples had the highest alginate content, 45.1, 43.8 and 42.6 %, respectively, while the lowest recorded contents were 12.25 % in *S. latissima* from the Faroe Islands. The vast majority of carbohydrates, and in a few cases over 40 % of the total DW of the seaweed, thus consisted of alginate, presenting a viable resource for industrial purposes.

The measured M/G ratios of most samples were relatively high, in the range of 2.4–7.0 (with individual outliers at 1.79 and 8.25). M/G ratios for alginate are typically reported in the range of 0.5–2.5 [21,23], however higher ratios above 6 have also been reported [25]. These high M/G ratios imply that resultant gel structures would be of low rigidity and high elasticity [19], favoring their use in situations where a high degree of structural rigidity is not necessary, such as biofilms and soft gels. There was a considerable difference in M/G ratio in different regions of origin, with *A. esculenta* from Bodø having an M/G ratio of 5.3, while the other *A. esculenta* samples ranged between 2.4 and 3.9 (Table 1). Also of note is that the three seaweeds with the highest alginate contents had very different M/G ratios, at 7.0, 3.9 and 3.0, respectively. All three of these seaweeds are comparably good sources of alginate, but of likely very differing properties due to stark differences in M/G ratio [19].

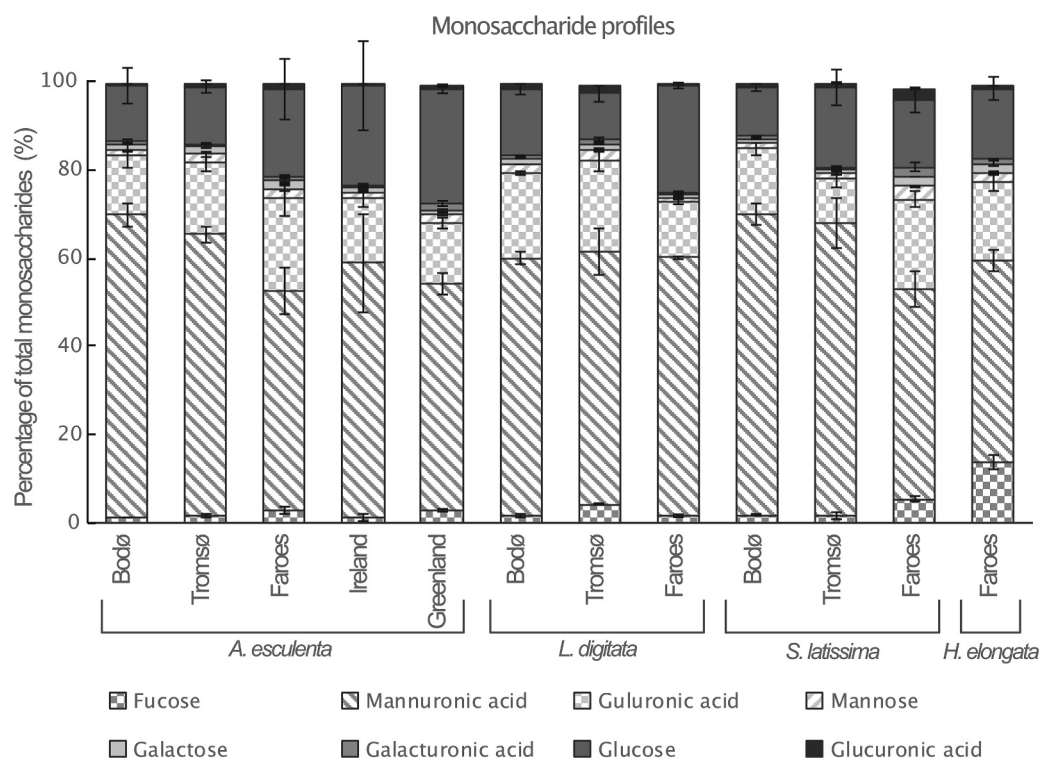


Fig. 1. Distribution of major monosaccharide species in brown seaweed. Monosaccharide profiles were measured by GC/MS, and are presented in terms of percentage of total monosaccharides. Error bars indicate standard deviation.

3.4. PLSR prediction of carbohydrate contents by infrared spectroscopies

PLSR modeling of NIR, DRIFTS and ATR spectra was used to predict carbohydrate contents in brown seaweed. For total carbohydrates, all three methods resulted in an RE of approx. 0.11, with NIR and ATR having an R^2 just below 0.8 and DRIFTS at just over 0.8 (Table 2). While having very slightly higher correlation between predicted and observed values, the DRIFTS method had the highest RMSEP at 5.72 with the other two both being approx. 5.2. None of the methods were successful in predicting crystalline cellulose contents, having relatively high predictive error and an R^2 between 0.2 and 0.3. This is likely due to the spectral signatures of cellulose being almost completely drowned out by overlapping absorbance bands of the far higher quantities of alginate, and the fact that cellulose lacks a unique spectral signature as it is not the only glucose-based polymer in the samples. The presence of other polysaccharides consisting of glucose thus makes it far more impractical to isolate crystalline cellulose from a complex spectrum. The potential difficulties of quantifying polysaccharides with overlapping spectral

Table 2

Prediction results from PLSR modeling of carbohydrate contents using different infrared spectroscopies.

Predicted quantity	Spectra	Comp. number ^a	RMSEP	RE	R^2
Carbohydrates	NIR	5	5.20	0.11	0.79
	DRIFTS	5	5.72	0.11	0.81
	ATR	5	5.21	0.11	0.79
Cellulose	NIR	3	1.16	0.29	0.24
	DRIFTS	2	1.14	0.26	0.21
	ATR	3	1.16	0.26	0.26
Alginate	NIR	3	6.75	0.19	0.52
	DRIFTS	6	4.89	0.12	0.82
	ATR	6	5.16	0.14	0.70
M:G ratio	NIR	5	0.70	0.19	0.68
	DRIFTS	5	0.81	0.16	0.74
	ATR	5	0.65	0.14	0.86

^a Comp. number indicates the number of PLSR components used in the model.

bands are well documented and it is known that multivariate methods can overcome these issues [34], but in this case the amount of crystalline cellulose is likely too low compared to the much more abundant alginate.

Prediction of alginate was most accurate when using DRIFTS, with RMSEP = 4.89, RE = 0.12 and $R^2 = 0.82$, while the other two methods had $R^2 < 0.8$ and higher predictive error. The higher accuracy of DRIFTS prediction of alginate and potentially total carbohydrates when compared to ATR can likely be explained by the fact that the ATR spectrum loses intensity at higher wavenumbers due to decreased sample penetration depth. DRIFTS spectra have more linear correlation between absorbance intensity and quantity of the measured analyte across the spectrum, so it is typically more capable of quantitative analysis. It is worth noting that for prediction of alginate, the NIR model incorporated far fewer components than the FTIR methods, meaning that the risk of overfitting is considerably lower but the model will also be far more simplistic and less comparable to the other models [35]. Using cross-validation, 3 components was calculated to be optimal for NIR while 6 components were calculated for the other two. For the sake of comparison, 6 components was also attempted for NIR modeling of alginate, but this resulted in far higher predictive error (RMSEP = 8.99, RE = 0.27, R^2 of prediction = 0.15), likely due to excessive overfitting. The best-performing model is thus reported in Table 2.

For prediction of M/G ratios, ATR proved most accurate with an RMSEP = 0.65, RE = 0.14 and $R^2 = 0.86$. The predicted M/G ratios correlated poorly to the expected ones when using the other two methods, both scoring $R^2 < 0.8$, and the prediction error was considerably higher than with ATR. This could be a potential advantage of the non-linear absorbance intensity of ATR, as it emphasizes bands in the lower wavenumbers of the fingerprint region, including those originating from glycosidic linkages in polysaccharides [34]. This region has more bands which are specific to poly-M or poly-G segments, so decreasing the proportional contribution from higher wavenumber regions could be the reason why ATR fared better in prediction of M/G ratios. The spectra shown in Fig. 2 indicate a clearer correlation between

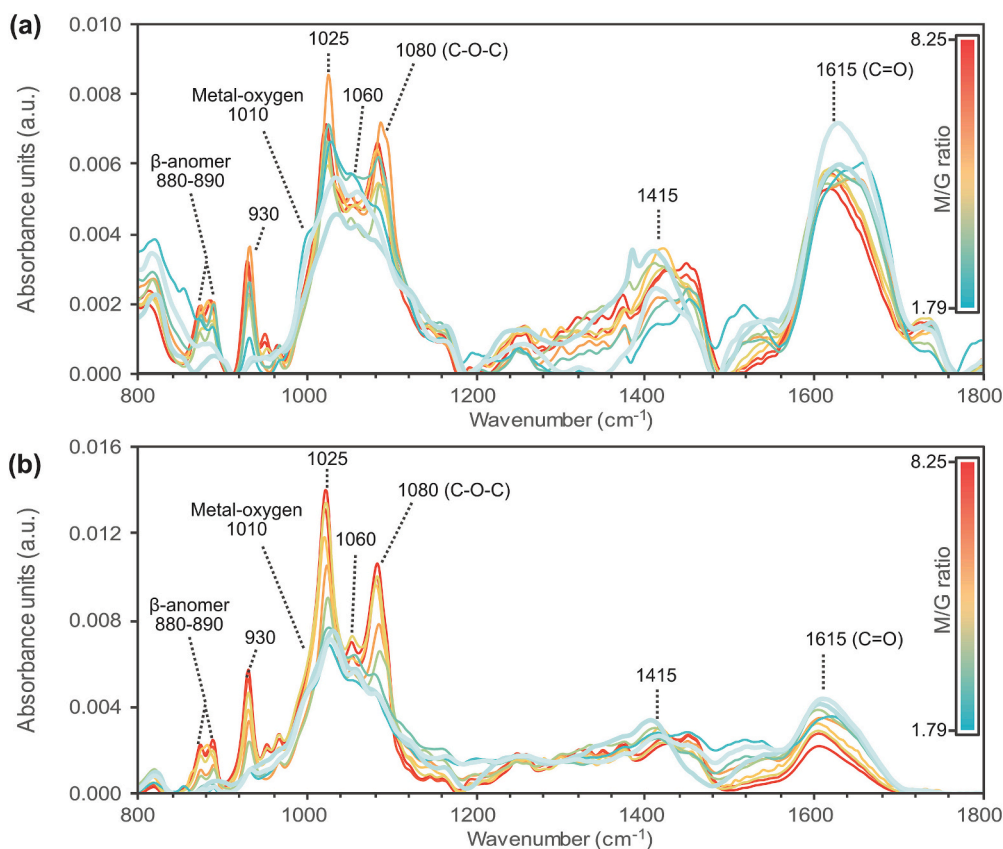


Fig. 2. The effect of differing M/G ratios on spectral FTIR absorbance in brown seaweed. (a) DRIFTS spectra and (b) ATR spectra. Potential absorbance bands which are relevant to determining M/G ratio or that are known to be associated with alginate are labeled. The heatmap indicates the M/G ratio of the sample, with red being the highest and blue being the lowest.

M/G ratios and the intensities of certain signature peaks in the lower wavenumbers than in DRIFTS.

The validity of PLSR analysis of spectral data can be verified by comparing the regression coefficients to the presence of bands which are expected to be relevant to predicting the analyte of interest [35]. PLSR coefficients should in principle show strong correlation to peaks in the spectrum which stem from the compound that is being predicted. If the coefficients contain numerous correlations to irrelevant spectral regions, this could be an indicator that the model has been overfitted. For NIR spectra, these coefficients are hard to interpret as they do not contain clearly resolved bands, but FTIR spectra on the other hand contain relatively specific absorbance signatures for specific molecular bonds and functional groups.

Regression coefficients for DRIFTS and ATR spectra indicated several relevant bands for determining alginate (Fig. 3). With both techniques, the band at 1615 cm^{-1} appeared highly correlated with alginate contents, as is to be expected due to the strong C=O vibrations of alginate in this spectral region [25]. The negative correlation to regions immediately above and below correspond to the Amide I and II bands of protein [36]. The coefficients also showed considerable contribution from areas in the $1100\text{--}1400\text{ cm}^{-1}$ range, which is a more amorphous region with very few assigned absorbance bands and thus harder to attribute to specific vibrational signatures. The ATR model also heavily emphasized the 1025 cm^{-1} peak, known to correlate to M [20], likely due to the aforementioned relative decrease in high-wavenumber intensities leading to emphasis of lower wavenumber bands.

Using FTIR spectra, PLSR coefficients indicate that two peaks at 880 and 890 cm^{-1} have particularly strong positive correlation to the M/G ratio (Fig. 3B). Peaks in this region are known to be indicative of β -anomeric bonds in saccharides [34], and has been suggested to distinguish M from G in alginate as well [23] since M-residues are β -D-

pyranoses while G residues are α -L-pyranoses. In Fig. 2, these bands do appear to increase in intensity and definition along with the increasing M/G ratio, and this appears to be reflected in previous studies of purified alginates as well [20,21].

Three absorbance bands in the $900\text{--}1100\text{ cm}^{-1}$ region (930 , 1025 and 1080 cm^{-1}) stand out as being highly pronounced in samples with high M/G ratios while almost being absent at the lowest recorded ratios. Firstly, the 930 cm^{-1} band increases notably in intensity and sharpness as M-content increases, although the ATR regression coefficient shows considerably lower dependence on this band than DRIFTS. To the authors' knowledge, this band has no previously described association to M content, but it has been shown to be a significant band in alginate and alginate-containing seaweed before [22]. The peak at 1025 cm^{-1} is related to C-O-C stretching in pyran rings [34] and has previously been shown to decrease in relation to a band at approx. 1010 cm^{-1} associated with metal-oxygen interactions, as the M/G ratio decreases [20]. While the 1010 cm^{-1} band is not clearly resolved in these spectra due to the complex composition of the seaweed biomass and the low G-contents of the studied seaweeds, it does appear to be present as a shoulder on the 1025 cm^{-1} peak, shifted closer to 1000 cm^{-1} (Fig. 2). Consistent with existing literature, this shoulder peak appears more pronounced in low M/G samples since there are more binding sites for metal ions in samples with a higher proportion of G-residues. When this shoulder peak increases, the 1025 cm^{-1} band decreases, as described previously by Sakugawa et al. [20].

The sharp peak at 1080 cm^{-1} is also attributed to C-O-C stretching in pyran rings [34], and has been described previously as being associated with both M and G residues, only changing slightly with different M/G ratios in purified alginate [20]. In the present study however, the intensity of this band appears highly dependent on the M/G ratio, as the band is very consistently of higher intensity at higher M/G ratios, while

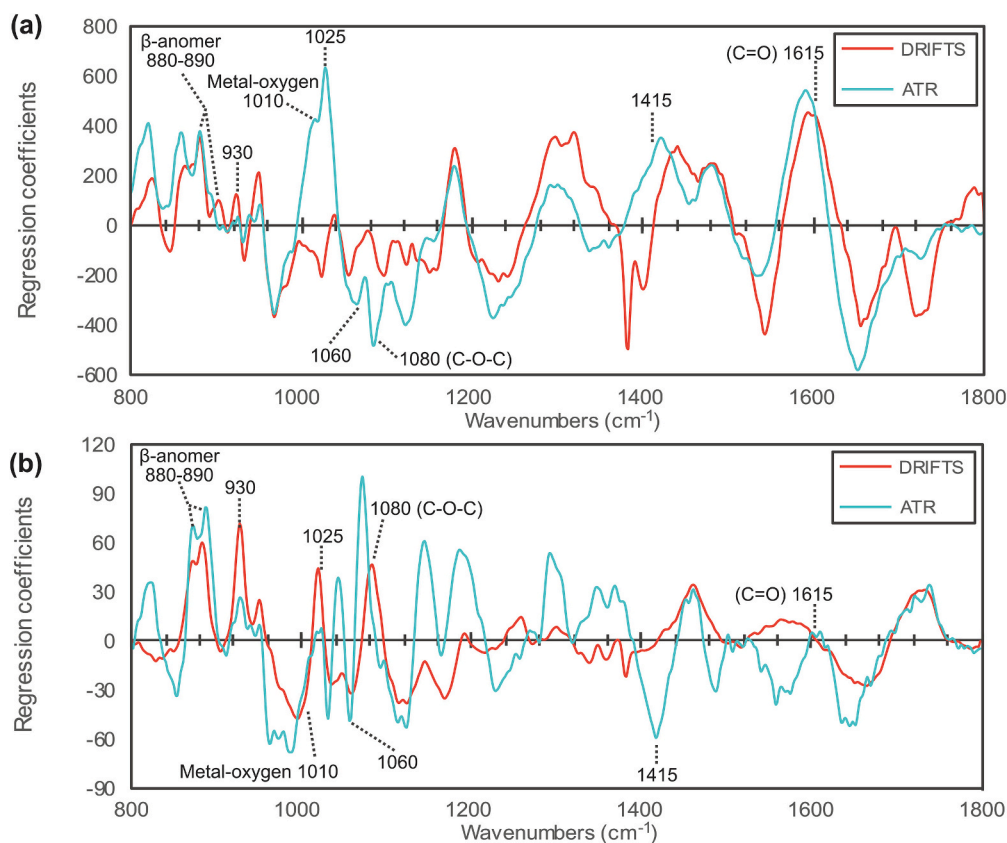


Fig. 3. Regression coefficients from PLSR prediction modeling. (a) Total alginate and (b) M/G ratios. Positive values imply positive correlation and negative values imply negative correlation to alginate contents or M/G ratio.

appearing almost absent in both DRIFTS and ATR spectra at the lowest recorded ratios (Fig. 2).

The regression coefficient for ATR indicates a strong negative correlation between M/G contents and a band at approx. 1415 cm^{-1} (Fig. 3B), while DRIFTS does not. There is a band in this area which has been observed in other FTIR analyses of alginate [22,23,25], and it is known that metal-carboxylate compounds have a low-intensity absorbance peak at these wavenumbers [37]. The ATR spectra show a slight increase in this band along with a significant shift towards lower wavenumbers at lower M/G ratios too, while the band is less defined in DRIFTS.

The peak ratios of individual absorbance bands in the FTIR-ATR spectrum have been previously used to achieve approximate estimations of M/G ratios in alginate [20,22]. Due to the complex nature of biological material like seaweed biomass however, the use of multivariate methods can improve the accuracy of prediction as they take into account a far wider array of absorbance signatures [38]. Importantly, the position of alginate's FTIR absorbance peaks are subject to shifts depending on which metal ion the polymer forms salts with [20]. The M/G ratio has been determined previously with good accuracy by calculating the ratio of band intensities at either 1030 and 1080 cm^{-1} or 1010 and 1025 cm^{-1} , depending on whether the alginate is in salt form with Ca^{2+} or Mg^{2+} , respectively [20]. This was done in purified alginate where the salt type was known however, which works very well, but in its natural form in the seaweed cell wall alginate tends to bind a variety of metals. This likely makes the peaks broader and less defined, in addition to potential overlap with bands from other compounds in the seaweed. Peaks might also be shifted in a more complex chemical environment compared to spectra of pure compounds, as can be seen in the present study where several peaks appear shifted compared to their expected positions. Thus, the PLSR method described here could provide a more accurate estimation of M/G ratio than peak ratio analysis by also

taking peak position into account. Beratto-Ramos et al. [39] showed that multivariate curve resolution-alternating least squares (MCR-ALS) could be used to isolate pure spectra of alginate and other polysaccharides from brown seaweed samples, and subsequently for determination of M/G ratio. PLSR has been previously shown by Jensen et al. [21] to be useful for M/G ratio determination in purified alginate, attaining very high accuracy of prediction ($\text{RMSEP} = 0.07$, $R^2 = 0.98$), while also being more reliable for prediction of M/G contents in alginate of different salt types. The present study further demonstrates the use of IR spectral analysis coupled with PLSR to determine M/G ratio directly in seaweed biomass, showing that its usefulness is not limited to extracted alginate.

4. Conclusions

The present study provides a detailed account of saccharide contents in North Atlantic brown seaweed of several different species by GC/MS analysis, including the identification and quantification of mannuronic acid and guluronic acid contents by this method. Further, it is shown that there is potential in using infrared spectroscopy coupled with PLSR analysis for the quantification of both total carbohydrates and alginate in brown seaweed biomass, but also for estimating the ratio of M and G residues in the alginate present in this biomass. This multivariate technique could have uses in the seaweed industry, as the M/G ratio heavily influences the properties of the extracted alginate and therefore its potential uses. With a larger data set of a wider range of species, a more complete, general model for prediction of M/G ratios in brown seaweed could be generated, and the technique could be used to predict alginate composition on a routine, large scale. Alternatively, to reduce interference from other compounds, species-specific models could be made which would likely offer higher accuracy but be useful for a narrower range of samples. ATR spectroscopy holds particular promise for future research as it is much less sensitive to moisture than DRIFTS is, and the

use of portable ATR spectrophotometers for direct M/G ratio estimation in wet seaweed could thus be highly useful for determining which seaweed could be used for further industrial processing. Spectral prediction methods also benefit from environmental sustainability due to requiring minimal or no chemical use, as well as being quick and simple to perform.

Supplementary data to this article can be found online at <https://doi.org/10.1016/j.ijbiomac.2023.127870>.

CRedit authorship contribution statement

Calle Niemi: Conceptualization, Methodology, Formal analysis, Investigation, Data Curation, Writing - Original Draft, Visualization.

Junko Takahashi: Methodology, data processing, Writing - Review & Editing.

Andr s Gorz s: Methodology, data processing, Writing - Review & Editing.

Francesco Gentili: Conceptualization, Methodology, Resources, Writing - Review & Editing, Supervision, Project administration, Funding acquisition.

Declaration of competing interest

The authors declare that they have no conflict of interest.

Data availability

Data will be made available on request.

Acknowledgements

Swedish Metabolomics Centre (SMC) for RDA (version 2016.09). The authors greatly appreciate the Northern Periphery and Arctic programme of the European Union SW-GROW project for financial support. The authors would like to thank Dr. Agnes Mols Mortensen at TARI – Faroe Seaweed, T rshavn, Faroe Islands, Dr. Ralf Rautenberger at the Department of Algae Production, Norwegian Institute of Bioeconomy Research (NIBIO), Bod , Norway and Dr. Sanna Matsson at M reforsking AS,  lesund, Norway from providing seaweed samples.

References

- R. Gade, M. Tulasi, V. Bhai, Seaweeds: a novel biomaterial, *Int J Pharm Pharm Sci* 5 (2013) 40–44.
- S. Mohamed, S.N. Hashim, H.A. Rahman, Seaweeds: a sustainable functional food for complementary and alternative therapy, *Trends Food Sci. Technol.* 23 (2) (2012) 83–96.
- L.-E. Rioux, S.L. Turgeon, Seaweed carbohydrates, in: *Seaweed Sustainability*, 2015, pp. 141–192.
- D. Oakenfull, M. Glicksman, Gelling agents, *C R C Crit. Rev. Food Sci. Nutr.* 26 (1) (2009) 1–25.
- J. Necas, L. Bartosikova, Carrageenan: a review, *Vet. Med.* 58 (4) (2013) 187–205.
- T. Helgerud, O. G ser d, T. Fj reide, P. Andersen, C. Larsen, *Alginates*, 2009, pp. 50–72.
- G.S. Anisha, S. Padmakumari, A.K. Patel, A. Pandey, R.R. Singhania, Fucoidan from marine macroalgae: biological actions and applications in regenerative medicine, drug delivery systems and food industry, *Bioengineering (Basel)* 9 (9) (2022).
- S. Karuppusamy, G. Rajauria, S. Fitzpatrick, H. Lyons, H. McMahon, J. Curtin, B. K. Tiwari, C. O'Donnell, Biological properties and health-promoting functions of laminarin: a comprehensive review of preclinical and clinical studies, *Mar. Drugs* 20 (12) (2022).
- A. Hurtado, A.A.A. Aljabali, V. Mishra, M.M. Tambuwala, A. Serrano-Aroca, Alginate: enhancement strategies for advanced applications, *Int. J. Mol. Sci.* 23 (9) (2022).
- E. Tavassoli-Kafrani, H. Shekarchizadeh, M. Masoudpour-Behabadi, Development of edible films and coatings from alginates and carrageenans, *Carbohydr. Polym.* 137 (2016) 360–374.
- G. Cervino, L. Fiorillo, A.S. Herford, L. Laino, G. Troiano, G. Amoroso, S. Crimi, M. Matarese, C. D'Amico, E. Nastro Siniscalchi, M. Cicciu, Alginate materials and dental impression technique: a current state of the art and application to dental practice, *Mar. Drugs* 17 (1) (2018).
- S. Mandal, G.K. Nagi, A.A. Corcoran, R. Agrawal, M. Dubey, R.W. Hunt, Algal polysaccharides for 3D printing: a review, *Carbohydr. Polym.* 300 (2023), 120267.
- B. Wang, P.J. Diaz-Payno, D.C. Browe, F.E. Freeman, J. Nulty, R. Burdis, D.J. Kelly, Affinity-bound growth factor within sulfated interpenetrating network bioinks for bioprinting cartilaginous tissues, *Acta Biomater.* 128 (2021) 130–142.
- K. Kanagesan, R. Abdulla, E. Derman, M.K. Sabullah, N. Govindan, J.A. Gansau, A sustainable approach to green algal bioplastics production from brown seaweeds of Sabah, Malaysia, *J. King Saud Univ. Sci.* 34 (7) (2022).
- F. Wang, X. Lu, X.Y. Li, Selective removals of heavy metals (Pb(2+), Cu(2+), and Cd(2+)) from wastewater by gelation with alginate for effective metal recovery, *J. Hazard. Mater.* 308 (2016) 75–83.
- J.-S. Yang, Y.-J. Xie, W. He, Research progress on chemical modification of alginate: a review, *Carbohydr. Polym.* 84 (1) (2011) 33–39.
- H. Porse, B. Rudolph, The seaweed hydrocolloid industry: 2016 updates, requirements, and outlook, *J. Appl. Phycol.* 29 (5) (2017) 2187–2200.
- P. Thiviya, A. Gamage, A. Liyanapathiranga, M. Makehelwala, R.S. Dassanayake, A. Manamperi, O. Merah, S. Mani, J.R. Koduru, T. Madhujith, Algal polysaccharides: structure, preparation and applications in food packaging, *Food Chem.* 405 (2023).
- M.J. Costa, A.M. Marques, L.M. Pastrana, J.A. Teixeira, S.M. Sillankorva, M. A. Cerqueira, Physicochemical properties of alginate-based films: effect of ionic crosslinking and mannuronic and guluronic acid ratio, *Food Hydrocoll.* 81 (2018) 442–448.
- K. Sakugawa, A. Ikeda, A. Takemura, H. Ono, Simplified method for estimation of composition of alginates by FTIR, *J. Appl. Polym. Sci.* 93 (3) (2004) 1372–1377.
- H.M. Jensen, F.H. Larsen, S.B. Engelsen, Characterization of alginates by nuclear magnetic resonance (NMR) and vibrational spectroscopy (IR, NIR, Raman) in combination with chemometrics, in: D.B. Stengel, S. Connan (Eds.), *Natural Products From Marine Algae: Methods and Protocols*, Springer New York, New York, NY, 2015, pp. 347–363.
- E. G mez-Ord nez, P. Rup rez, FTIR-ATR spectroscopy as a tool for polysaccharide identification in edible brown and red seaweeds, *Food Hydrocoll.* 25 (6) (2011) 1514–1520.
- N. Chandia, Alginic acids in *Lessonia trabeculata*: characterization by formic acid hydrolysis and FT-IR spectroscopy, *Carbohydr. Polym.* 46 (1) (2001) 81–87.
- D. Rodrigues, A.C. Freitas, L. Pereira, T.A. Rocha-Santos, M.W. Vasconcelos, M. Roriz, L.M. Rodriguez-Alcala, A.M. Gomes, A.C. Duarte, Chemical composition of red, brown and green macroalgae from Buarcos bay in Central West Coast of Portugal, *Food Chem.* 183 (2015) 197–207.
- W. Jiao, W. Chen, Y. Mei, Y. Yun, B. Wang, Q. Zhong, H. Chen, W. Chen, Effects of molecular weight and guluronic acid/mannuronic acid ratio on the rheological behavior and stabilizing property of sodium alginate, *Molecules* 24 (23) (2019).
- M.Z.I. Mollah, M.R.I. Faruque, D.A. Bradley, M.U. Khandaker, S.A. Assaf, FTIR and rheology study of alginate samples: effect of radiation, *Radiat. Phys. Chem.* 202 (2023).
- C. Niemi, A.M. Mortensen, R. Rautenberger, S. Matsson, A. Gorz s, F.G. Gentili, Rapid and accurate determination of protein content in North Atlantic seaweed by NIR and FTIR spectroscopies, *Food Chem.* 404 (Pt B) (2023), 134700.
- D.M. Updegraff, Semimicro determination of cellulose in biological materials, *Anal. Biochem.* 32 (3) (1969) 420–424.
- J.F. Saeman, Kinetics of wood saccharification - hydrolysis of cellulose and decomposition of sugars in dilute acid at high temperature, *Ind. Eng. Chem.* 37 (1) (1945) 43–52.
- C.C. Sweeley, R. Bentley, M. Makita, W.W. Wells, Gas-liquid chromatography of trimethylsilyl derivatives of sugars and related substances, *J. Am. Chem. Soc.* 85 (16) (1963) 2497–2507.
- A. Gorz s, B. Sundberg, Chemical fingerprinting of Arabidopsis using Fourier transform infrared (FT-IR) spectroscopic approaches, *Methods Mol. Biol.* 1062 (2014) 317–352.
- M. Kaur, M. Kumar, S. Sachdeva, S.K. Puri, Aquatic weeds as the next generation feedstock for sustainable bioenergy production, *Bioresour. Technol.* 251 (2018) 390–402.
- G. Michel, T. Tonon, D. Scornet, J.M. Cock, B. Kloareg, Central and storage carbon metabolism of the brown alga *Ectocarpus siliculosus*: insights into the origin and evolution of storage carbohydrates in Eukaryotes, *New Phytol.* 188 (1) (2010) 67–81.
- T. Hong, J.Y. Yin, S.P. Nie, M.Y. Xie, Applications of infrared spectroscopy in polysaccharide structural analysis: Progress, challenge and perspective, *Food Chem. X* 12 (2021), 100168.
- A.A. Gowen, G. Downey, C. Esquerre, C.P. O'Donnell, Preventing over-fitting in PLS calibration models of near-infrared (NIR) spectroscopy data using regression coefficients, *J. Chemom.* 25 (7) (2011) 375–381.
- J. Schmitt, H.-C. Flemming, FTIR-spectroscopy in microbial and material analysis, *Int. Biodegradat. Biodegradat.* 41 (1) (1998) 1–11.
- E.G. Palacios, G. Ju rez-L pez, A.J. Monhemius, Infrared spectroscopy of metal carboxylates, *Hydrometallurgy* 72 (1–2) (2004) 139–148.
- C.J. Strachan, T. Rades, K.C. Gordon, J. Rantanen, Raman spectroscopy for quantitative analysis of pharmaceutical solids, *J. Pharm. Pharmacol.* 59 (2) (2007) 179–192.
- A. Beratto-Ramos, C. Agurto, J. Vargas, R. Castillo, Fourier-transform infrared imaging and multivariate analysis for direct identification of principal polysaccharides in brown seaweeds, *Carbohydr. Polym.* 230 (2019).